Applied Thermal Engineering 126 (2017) 920–928

Contents lists available at ScienceDirect

Applied Thermal Engineering

journal homepage: www.elsevier.com/locate/apthermeng

Research Paper

Thermal and hydraulic performance of a compact plate finned tube air-fuel heat exchanger for aero-engine

Jie Wen [a,b], Haoran Huang [a,*], Haiwang Li [a,b,c], Guoqiang Xu [a,b], Yanchen Fu [a]

[a] National Key Laboratory of Science and Technology on Aero Engines Aero-thermodynamics, Beihang University, Beijing 100191, China
[b] The Collaborative Innovation Center for Advanced Aero-Engine of China, Beihang University, Beijing 100191, China
[c] Aircraft/Engine Integrated System Safety Beijing Key Laboratory, Beihang University, Beijing 100191, China

HIGHLIGHTS

- A compact finned tube heat exchanger with small tube diameter and light weight was designed and optimized.
- An efficient method of manufacturing finned tube heat exchanger with thin tube was introduced.
- Correlation factors are proposed to correct the pressure difference calculation error based on experiments.
- An empirical relationship for outside heat transfer of finned tube heat exchanger is developed.

ARTICLE INFO

Article history:
Received 25 January 2017
Revised 20 June 2017
Accepted 14 July 2017
Available online 15 July 2017

Keywords:
Finned tube heat exchanger
Air-fuel heat exchanger
LMTD
Aero-engine
Heat transfer empirical correlation

ABSTRACT

The article presents a novel compact plate finned-tube air-fuel heat exchanger which is designed by means of using logarithmic mean temperature difference method (LMTD) and both thermal and hydraulic performance of the heat exchanger are experimentally investigated. Worldwide, due to the harsh working condition, both aviation industry and aerospace industry department are in badly need of compact heat exchanger with light weight and high efficiency. In this paper, the design, manufacture and tests of a prototype, plate finned tube heat exchanger are presented. The stainless-steel heat exchanger weights 1.207 kg and by using the fuel RP-3 as the coolant, it can cool the high-temperature air from high pressure compressor in aircraft engine in a very limited space. The study of flow resistance in air-fuel flow allows determining the flow friction factor. Experimental values of heat transfer for the heat exchanger are also calculated. In addition, obtained values of heat transfer coefficient show some differences with literature correlations. Based on these differences, an empirical correlation for the outside heat transfer of compact finned tube heat exchanger is established, which will be helpful for the researchers to design similar heat exchangers.

1. Introduction

The speed of aircraft has increased from subsonic to supersonic over the last decades because of the advent and development of the aircraft jet engine. Recently, the technologic research on the aerospace plane made a higher demand of speed (up to 5 Mach) and as the result, the engine for hypersonic aircraft become a challenge of 21st century. For modern gas turbine engines, to achieve higher thermal efficiency, increasing turbine inlet temperature (T_3^*) and increasing compressor pressure ratio on this basis are most widely used methods. With the development of engine technology, current turbine inlet temperature is far beyond the allowable metal temperatures, which is approaching 2000 K. As the base material development lagged behind the demand of practical application, turbine inlet temperature can only be increased further by using highly sophisticated cooling techniques [1]. Several effective cooling technologies including convective cooling, film cooling and impingement cooling have been successfully introduced to cool high-temperature components for the last decades. Han et al. [2] have detailed described the available advanced cooling techniques applied in the gas turbine industry.

However, though all the above three cooling technologies are effective, they have the same disadvantage; that is, they all need high pressure air from high pressure compressor. On the one hand, because of high stagnation temperature brought about by the high speed, the compressor bleed air is quiet too hot to be used as coolant [3], and on the other hand, efficiency considerations of engine

* Corresponding author.
E-mail address: haoran_huang@buaa.edu.cn (H. Huang).

http://dx.doi.org/10.1016/j.applthermaleng.2017.07.103
1359-4311/

Nomenclature

A	heat transfer area (m^2)
A_r	tube area of fin side (m^2)
A_t	total area of fin side (m^2)
c_p	isobaric specific heat capacity ($J\ kg^{-1}\ K^{-1}$)
d	diameter (m)
d_e	equivalent outer diameter (m)
f	friction factor (–)
f_c	corrected friction factor (–)
G_{max}	mass flow of the air based on the minimum flow area ($kg\ s^{-1}\ m^{-2}$)
h	heat transfer coefficient ($W\ m^{-2}\ K^{-1}$)
K	overall heat transfer coefficient ($W\ m^{-2}\ K^{-1}$)
l	total length (m)
m	parameter of calculating fin efficiency
$\dot{m}$	mass flow ($kg\ s^{-1}$)
N	elbow number (–)
n	fin number (–)
P	pressure (Pa)
ΔP	pressure difference (Pa)
Δp_j	flow resistance due to inlet and outlet pipe connection (Pa)
Δp_L	distance flow resistance (Pa)
Δp_r	flow resistance due to return flow (Pa)
Q	total heat transfer rate (W)
R_{eq}	equivalent radius of circular fin (m)
r	radius (m)
S	fin pitch (m)
S_1	transverse tube pitch (m)
S_2	longitudinal tube pitch (m)
T	temperature (K)
ΔT_m	logarithmic mean temperature difference (K)
u	velocity ($m\ s^{-1}$)

Dimensionless quantity

Nu	Nusselt number
Pr	Prandtl number
Re	Reynolds number

Abbreviation

CCA	cooled cooling air
HPC	high pressure compressor
HTC	heat transfer coefficient
LMTD	logarithmic mean temperature difference method

Greek symbols

φ	temperature difference correction factor
λ	thermal conductivity ($W\ m^{-1}\ K^{-1}$)
ρ	density ($kg\ m^3$)
μ	dynamic viscosity (Pa s)
ϕ	parameter of calculating fin efficiency
δ	fin thickness
η	fin efficiency
ξ	Filonenko flow resistance coefficient

Subscripts

c	cold or cold side
cal	calculation
exp	experimental
f	fin or fin side
h	hot or hot side
i	inside or inlet
o	outside or outlet
s	stainless steel
w	wall

demand accomplishing cooling with minimum amount of cooling air which conflict with the application of cooling that large cooling air are required. Besides, geometric constraints in combination with aerodynamic demands are also challenging to an adequate cooling [4]. Consequently, a new concept of cooling is demanded urgently.

To balance the contradiction between efficiency and cooling, a kind of new technology, called cooled cooling air (CCA in short) technology, was employed. The application of CCA allows cold fuel with high heat capacity cooling hot air in a nearby fuel-air heat exchanger, and then fuel can be nebulized better for further efficient combustion [5]. The heat transfer is accomplished in air-fuel heat exchanger, so it is significant to do detailed research on the design, manufacture and performance of compact heat exchanger.

Literature surveys indicated that there were many researchers investigated both compact heat exchanger and heat exchanger used in aircraft. MTU Aero Engines and Aristotle University of Thessaloniki has made many efforts on both experimental and numerical investigation of a novel air-air heat exchanger with U-shaped elliptic profiled tubes [6–8]. The heat exchanger allows heat transfer between hot exhausted gas from turbine and air from high pressure compressor and recovers waste heat from high temperature gas. By using elliptically profiled tubes of staggered arrangement, high heat transfer effectiveness is combined with minimum aerodynamic pressure losses. As a consequence, the novel heat exchanger can not only save energy and improve effectiveness but also reduce NOx emissions and noise level. Muszynski and Andrzejczyk carried experimental studies on a compact heat exchanger by impinging microjet [9]. In their works, a prototype impingement cooling heat exchanger was manufactured and tested. It is found that the overall heat transfer coefficient (HTC) reached over 10000 W/m^2 K, and they also compared the obtained HTC with literature correlations. The results show differences between HTC predicted by literature correlations and experiments. Authors also proposed their own empirical correlation for jet impingement HTC.

However, in the experiments and analysis of air-fuel heat exchanger using in aircraft, because of the high heat transfer coefficient between tube wall and fuel, it is found that the air side thermal resistance is several times, sometimes more than ten times larger than that of fuel side. Therefore compared with improving the heat transfer performance of fuel side, it is more efficient to improve the air side. As a consequence, enhanced surfaces are employed to decrease thermal resistance of air side. Various research has been conducted on different fin patterns and geometries. Wang [10,11] presented several surveys and summarized the development of finned tube heat exchanger patents during 1981–1999 and 2001–2009. In the surveys a total of 74 patents including plate, wavy, louver, slit, vortex generators and other special and creative fin patterns were examined. Also, the authors provided some explanations about how the special fin patterns work. At the end of the papers, the author recommended more detailed numerical simulation and experimental investigation to gain fur-

ther insight to finned tube heat exchanger designs. Han et al. [12,14] carried a numerical investigation on finned tube heat exchanger with circular and oval tubes. There are three kinds of tubes were applied with wavy fin and louvered fin. The simulation found that the using of oval finned tube could improve the fin efficiency and then increase the heat transfer rate by 1.5–4.9%, while the pressure drop loss decreased by 22–31.8% at the same time. Liu et al. [13] also performed a numerical study on the air-side heat transfer enhancement for a finned tube heat exchangers with large fin pitches by using perforated fins. After investigating four perforated fins with different geometry structure, it was found that compared with plate finned tube heat exchanger without perforations, an optimal perforation design can be obtained to realize maximum increase in the heat transfer for the perforated heat exchanger.

Besides numerical simulation, there are also many experimental research and comparisons between simulated results and experimental results on finned tube heat exchanger. Wang and Chi [14,15] did research on the air side performance of plate finned tube heat exchanger and a total of 18 samples were tested. The study examined the effect of tube diameter, fin pitch and number of tube row on heat transfer and hydraulic characteristics. It is found that the heat transfer characteristics were significantly related to the fin pitch depending on the number of tube rows, but for the same fin pitch, the number of tube rows affects the friction performance little. The effect of tube diameter on heat transfer is also related to fin pitch. In addition, a correlation for plate finned tube heat exchanger is proposed. It is indicated that the proposed friction correlation can correlate 85.1% of the database within ±15% while the heat transfer correlation describes 88.6% of the database within ±15%. Jang and Yang [16] studied fluid flow and heat transfer over a finned tube heat exchanger experimentally and numerically. Three types of finned tube configurations have been investigated for different inlet velocity under wet and dry conditions. The results show that the average heat transfer coefficient of the elliptic tube is 35–50% of the corresponding circular tube with the same tube diameter while the pressure loss is only 25–30%. The numerical results of pressure loss for dry coils show good agreement with experimental data, while they overestimate the heat transfer coefficient by 30%. As a result, the author recommends serious consideration of variable tube surface temperature for each row and conjugate heat transfer between the tube and fin in the future.

In the study and application of heat exchanger using fuel as coolant, many researchers focus on flow resistance and heat transfer characteristics of fuel side [17–19], but study on air side is relatively small. In addition, as pointed out by Wang et al. [14], for ordinary industrial application, the use of decreased diameter tube, smaller longitudinal tube pitch and smaller transverse tube pitch in finned tube heat exchanger are popular since it could improve the thermal and hydraulic characteristics and save resources significantly. The smaller tube diameter means lower weight and higher compactness for a heat exchanger, which are the most worth considering for aircraft and aero-engine application. Unfortunately, most of the previous research mainly focus on those larger tube diameter (outer diameter larger than 6.7 mm), and the database containing smaller diameter have not been widely studied [15,20]. What's more, most heat exchanger researchers claimed that contact thermal resistance is negligible and the uncertainties are acceptable in their investigations. However, few researcher presented that their basis for small contact thermal resistance is justified, and the method of tube expansion is rarely mentioned [21].

This paper presents a novel compact plate finned tube air-fuel heat exchanger with thin tubes (with outer diameter = 2.2 mm) which is designed using logarithmic mean temperature difference method (LMTD). The manufacturing method of the heat exchanger is introduced in detail, and the reason why contact thermal resistance can be neglected is presented. Also, both thermal and hydraulic performance of the finned tube heat exchanger is experimentally investigated and the difference between experimental results and literature correlations is studied. Authors also proposed their empirical correlation for finned tube heat exchanger with thin tubes.

2. Heat exchanger design

The Logarithmic Mean Temperature Difference Method (LMTD) is widely applied to heat exchanger design and the finned tube heat exchanger mentioned in the paper is also designed by using LMTD. The method was introduced by Kay and Nedderman in their book [22] and it will not be repeated in detail here.

In the heat exchanger, the outside fluid is hot air from HPC (simulated by heated air in experiments) and the inside fluid is kerosene RP-3, which is the most common aviation fuel in China. Fluid properties of hot side air used in design calculation including density, thermal conductivity, dynamic viscosity and isobaric specific heat capacity are determined using EES [23] and properties of cold side fuel RP-3 refer to the data presented by Deng and Xu et al. [24–27].

The research object is a finned tube heat exchanger with inlined arrangement. As illustrated in Fig. 1, the essential core of the heat exchanger is a series snake tubes with plate fins. The tubes, fins and headers were all made of stainless steel Type 304 and the heat exchanger was with 268 mm in length, 72 mm in width and 80 mm in height, respectively. In order to meet the demands of aviation use, the air side flow resistance and heat exchanger weight are strictly limited, so tubes with the small outer diameter of 2.2 mm and the inner diameter of 1.8 mm and fins with a thickness of 0.5 mm were selected. As a consequence, with the fin pitch of 3 mm, the surface area density of the heat exchanger based on outside heat transfer area can be up to 697 m^2/m^3. The total weight of the heat exchanger is 1.207 kg.

3. Experimental apparatus

3.1. Manufacture of heat exchanger

Because of the small diameter and wall thickness of tubes, the method of mechanical expanding cannot be used in finned tube manufacture, or it is easy to cause damage to tubes. Consequently, the brazing method was chosen. Fig. 2 shows the process of finned tube heat exchanger manufacture. First, many U-shaped tubes with the outer diameter of 2.2 mm and the inner diameter of 1.8 mm were made and then fins and solder sheets were put on tubes. In this step, every fin has a solder sheet on it so that the solder can melt and infiltrate into the gap between tube and fin when brazing in a furnace, and this method can significantly decrease contact thermal resistance between tube and fin. Next, another type of U-shaped tube with the outer diameter of 1.8mm and the inner diameter of 1.5 mm were made and then inserted into the thick tubes. After that, the tubes are compressed by two plate and then headers are combined with the tubes. Finally, the gaps between thin elbows and thick tubes were coated with solder, and then the whole heat exchanger was brazed in a vacuum furnace under the temperature of 1040 °C for 12 h. After the brazing, the tubes of heat exchanger is filled with water and pressurized to 6 MPa to ensure that the brazing quality is good enough. The photos of manufacture are shown in Fig. 3.

Because of the diameter decrease of the elbows, the flow resistance is definitely changed with it, so it is significant to analyze the

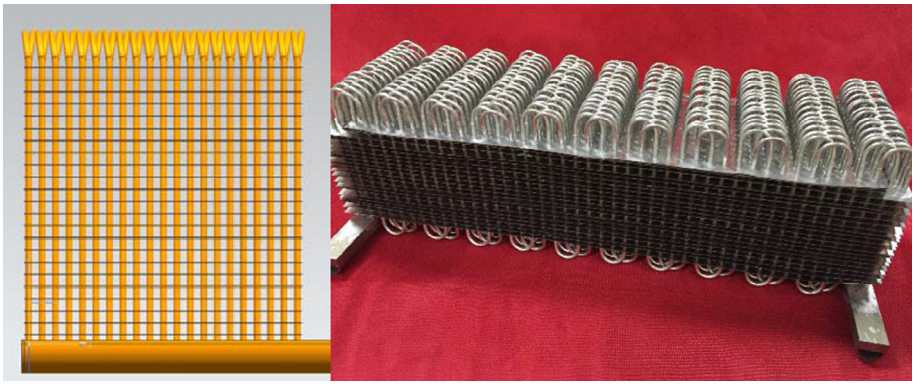

Fig. 1. Schematic and photo of finned tube heat exchanger.

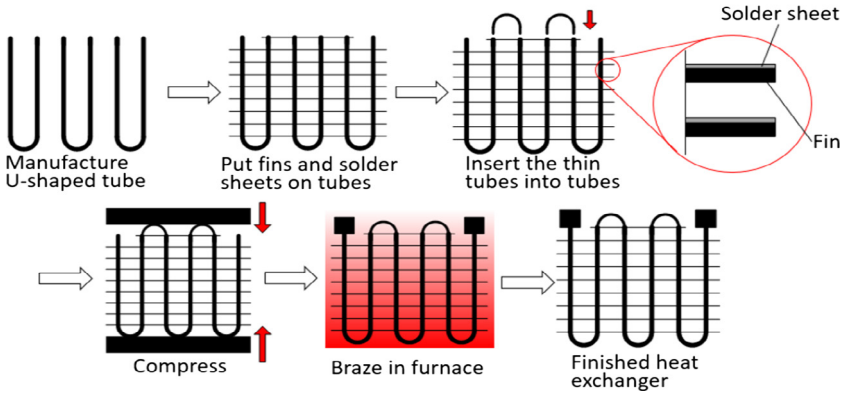

Fig. 2. Schematic of heat exchanger manufacture.

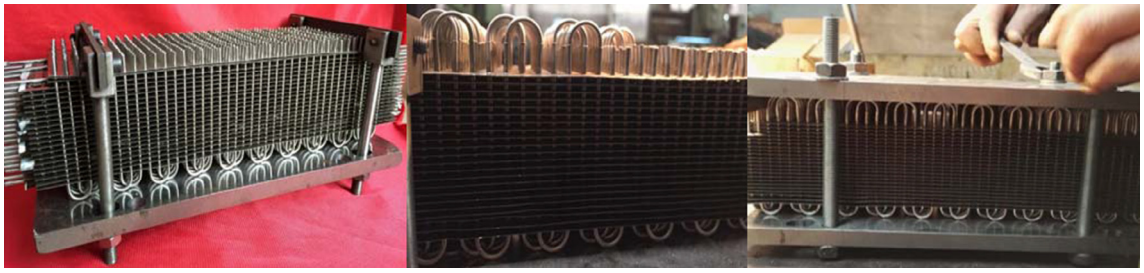

Fig. 3. Photos of heat exchanger manufacture.

pressure loss of the tubes carefully. The detailed discussion will be presented in Section 5.1.

3.2. Test rig

The experimental study was conducted on a heat exchanger test rig built in the National Key Laboratory of Science and Technology on Aero-engines Aero-thermodynamics at Beihang University, China. Apparatus allows to gather data regarding convective heat transfer between air and liquid or between air and air.

The present research shows results of steady state heat transfer and hydraulic experiments, conducted for single phase cooling. The test rig includes a high-temperature air loop and a low-temperature fuel loop. As shown in Fig. 4, the two loops provide heated air and cold fuel to simulate HPC bleed air (with high temperature) and fuel from the fuel tank (with low temperature), respectively. Both loops consist of the heat exchanger, fluid supplying system, water cooling system and several measuring devices. In air loop, desired fluid flow rate was obtained using a pneumatic flow control valve and measured accurately by an FCI thermal flow meter. Then in order to simulate hot air from HPC, the air passed through an electric heater and was heated from environment temperature to up to 250 °C with the temperature fluctuation of less than 1 °C. Exiting the heater, the hot air entered a 4 m long straight tube to ensure uniform and then flowed into the heat exchanger. After flowing out of the heat exchanger, hot air was cooled and exhausted to atmosphere. Just similar to the air loop, in the other loop fuel in room temperature flowed through a filter, and then was pressurized by a precision plunger pump so that the flow rate can be controlled accurately. The mass flow rate of fuel was measured by a Coriolis mass flow meter. After heat transfer in heat exchanger, the coolant fuel was cooled by a cooler and flowed back to fuel tank. The temperature was measured at inlets and outlets of heat exchanger and absolute pressure of inlets differential pressure

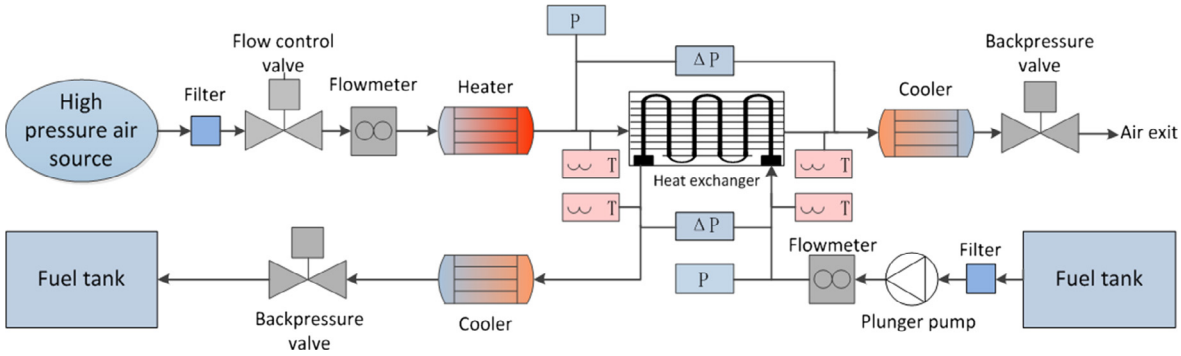

Fig. 4. Schematic of experimental system.

between inlets and outlets were also measured. The accuracy of temperature and pressure measurement will be introduced in Section 3.3.

Experimental measurement data were collected by ADAM 4018 and 4520, and they are connected to an automatic data acquisition set so that the data can be processed and analyzed easily.

In the experiments, the test section was covered by porous heat insulation materials with low thermal conductivity to reduce heat loss.

3.3. Measurement

The air side and fuel side flow rates are measured by a thermal flow meter and a Coriolis mass flow meter, respectively. The FCI thermal flow meter is with ±0.5% accuracy of reading value with measuring range of 0–0.5 kg/s and the SINCERITY Coriolis mass flow meter is with ±0.2% accuracy and 0–1.2 kg/s range.

In both air and fuel loop, pressures are measured by Rosemount pressure transmitter with accuracies of 0.25% and 0.04% of the full-scale reading, respectively. At the inlet of air side absolute pressure transmitter with a measuring range 0–0.8 MPa is amounted and for fuel side the range of another transmitter is 0–10 MPa. Two differential pressure transmitter are installed to measure the heat exchanger pressure loss of air side and fuel side with the range 0–6kPa and 0–0.6 MPa, respectively.

Temperatures were measured by several K type sheathed thermocouples, and all the thermocouples are pre-calibrated in an oil bath from 20 °C to 280 °C. It was found that the thermocouples are with an accuracy of ±0.6 K.

In the experiments, we waited for at least 5 min with all temperature, pressure and mass flow rate kept unchanged before recording experimental data.

4. Data reduction

To analyze the hydraulic and heat transfer performance of the finned tube heat exchanger, pressure loss and heat transfer coefficient have been calculated by using direct experimental measurements. Moreover, friction factor and Nusselt number are also presented.

The total amount of heat transferred can be written as:

$$Q = K_i A_i \Delta T_m \tag{1}$$

The logarithmic mean temperature difference can be used as temperature gradient between hot side air and cold side fuel. It can be written as:

$$\Delta T_m = \frac{(T_{h,i} - T_{c,o}) - (T_{h,o} - T_{c,i})}{\ln(T_{h,i} - T_{c,o}) - \ln(T_{h,o} - T_{c,i})} \tag{2}$$

Because of a higher measurement accuracy of Coriolis mass flow meter, the fuel side amount of heat transferred is considered to be more reliable (actually the amount of heat transfer difference between air side and fuel side is less than 3% in all cases). Consequently, the total amount of heat transferred can be calculated by temperature increase of fuel side:

$$Q = \dot{m}_c c_{pc}(T_{c,o} - T_{c,i}) \tag{3}$$

For finned tube heat exchanger, the overall heat transfer coefficient based on inside area is as follow:

$$\frac{1}{K_i} = \frac{1}{h_i} + \frac{d_i}{2\lambda_s}\ln\left(\frac{d_o}{d_i}\right) + \frac{A_i}{h_o(A_r + \eta A_f)} \tag{4}$$

where η denotes fin efficiency and it is calculated by the approximation method described by Schmidt [28].

$$\eta = \frac{\tanh(mr_o\phi)}{mr_o\phi} \tag{5}$$

where

$$m = \sqrt{\frac{2h_f}{\lambda_s \delta}} \tag{6}$$

$$\phi = \left(\frac{R_{eq}}{r_o} - 1\right)\left[1 + 0.35ln\left(\frac{R_{eq}}{r_o}\right)\right] \tag{7}$$

$$\frac{R_{eq}}{r_o} = 0.64\frac{S_1}{r_o}\left(\frac{S_2}{S_1} - 0.2\right) \tag{8}$$

The cold side heat transfer coefficient h_i is evaluated from the Gnielinski semi-empirical correlation [29]:

$$Nu_i = \frac{h_i d_i}{\lambda} = \frac{(\xi/8)Pr_i(Re_i - 1000)}{1 + 12.7\sqrt{\xi/8}(Pr_i^{2/3} - 1)}\left[1 + \left(\frac{d_i}{l}\right)^{2/3}\right] \tag{9}$$

where

$$\xi = (1.82\lg Re_i - 1.64)^{-2} \tag{10}$$

where $Re_i = \frac{\rho u_i d_i}{\mu}$ and $Pr_i = \frac{c_p \mu}{\lambda}$.

Combining Eqs. (1)–(4) and (9), the hot side heat transfer coefficient h_o and Nusselt number $Nu_o = \frac{h_o d_o}{\lambda}$ can be calculated.

The average temperature of inlet and outlet is used to estimate thermophysical properties for both air side and fuel side.

Based on Eq. (4), the uncertainty of heat transfer coefficient h_o can be calculated:

$$\frac{\Delta\left(\frac{A_i}{h_0(A_r+\eta A_f)}\right)}{\frac{A_i}{h_0(A_r+\eta A_f)}} = \sqrt{\left[\frac{\Delta(K_i)}{K_i}\right]^2 + \left[\frac{\Delta(h_i)}{h_i}\right]^2 + \left[\frac{\Delta\left(\frac{d_i}{2\lambda_s} ln\frac{d_o}{d_i}\right)}{\frac{d_i}{2\lambda_s} ln\frac{d_o}{d_i}}\right]^2} = 8.62\% \quad (11)$$

and $\frac{\Delta(h_o)}{h_o}$ was estimated to lower than 10%.

5. Results and discussion

As previously mentioned, the heated air was used to simulate HPC bleed air in aircraft engine, and the heat of the air is carried away by fuel. Experiments were performed to test flow resistance and heat transfer performance of the heat exchanger. In the experiments, the inlet temperature and mass flow rates of air and fuel changes respectively to cover as wide a range of experimental parameters as possible.

5.1. Flow resistance

Because tube bypass effects substantially degrade the inline tube arrangement, little use exists for finned tube heat exchanger of inline geometry. However, Shi et al. [30] introduced a correlation for inline arrangement which is developed by Vampola. The Vampola pressure difference is as follow:

$$\Delta p_o = f_o * \frac{nG_{max}^2}{2\rho} \quad (12)$$

where

$$f_o = 1.463\left(\frac{G_{max}d_e}{\mu}\right)^{-0.245}\left(\frac{S_1-d_o}{d_o}\right)^{-0.9}\left(\frac{S_1-d_o}{S}+1\right)^{0.7}\left(\frac{d_e}{d_o}\right)^{0.9} \quad (13)$$

Fig. 5 shows the pressure loss of hot side at different mass flow rates, where the pressure loss is defined as:

$$\text{pressure loss} = \frac{\Delta p_h}{p_{h,i}} \quad (14)$$

In the figure, the red point and line present the calculated pressure loss by using Vampola correlation and the black line present the experiments. It can be seen clearly that the calculated Vampola pressure losses are higher than the experimental data. Obvious discrepancies between experiments and calculation are visible. However, the change of experimental pressure loss with air mass flow give a similar trend as the pressure loss calculated by Vampola correlation. The difference may be attributed to different tube diameter. For plate finned tube heat exchanger, previous research mainly focus on tubes with large diameter and consequently, large tube pitch (outer diameter >6 mm, and $S_1 > 12.7$ mm [14]), but outer diameter of tubes in this paper is 2.2 mm and S_1 of the heat exchanger is 4.4 mm, which is much smaller than the most studied scale. As the result, the flow pattern in small scale is not clear enough yet, which may cause difference between results predicted by conventional correlation and experimental data.

Based on the difference, a correction factor for Vampola pressure difference is proposed:

$$f_{c,o} = 0.44 f_o \quad (15)$$

For hot side, the percentage of pressure loss error is defined as:

$$\text{Hot side pressure loss error} = \frac{\Delta p_{o,cal} - \Delta p_{o,exp}}{\Delta p_{o,exp}} \quad (16)$$

As shown in Fig. 6, after taking the correction factor 0.44 into consideration, the difference between calculated and experimental pressure loss is less than 4.5%.

Similar to the hot side, the pressure loss of cold side is defined as:

$$\text{pressure loss} = \frac{\Delta p_c}{p_{c,i}} \quad (17)$$

As recommended by Shi et al. in their book [30], the cold side pressure difference can be calculated by following equations:

$$\Delta p_i = \Delta p_L + \Delta p_r + \Delta p_j \quad (18)$$

where

$$\Delta p_L = \frac{0.3164}{Re_i^{0.25}}\frac{l}{d_i}\frac{\rho u_i^2}{2} \quad (19)$$

$$\Delta p_r = 1.3\frac{\rho u_i^2}{2}N \quad (20)$$

$$\Delta p_j = \rho u_i^2 \quad (21)$$

the equation means that the total inside pressure difference consists of three parts: pressure difference along the tube, pressure difference due to return flow in elbows, and pressure difference due to inlet and outlet pipe connection. However, as mentioned in Section 3.1, the flow resistance change definitely with the diameter

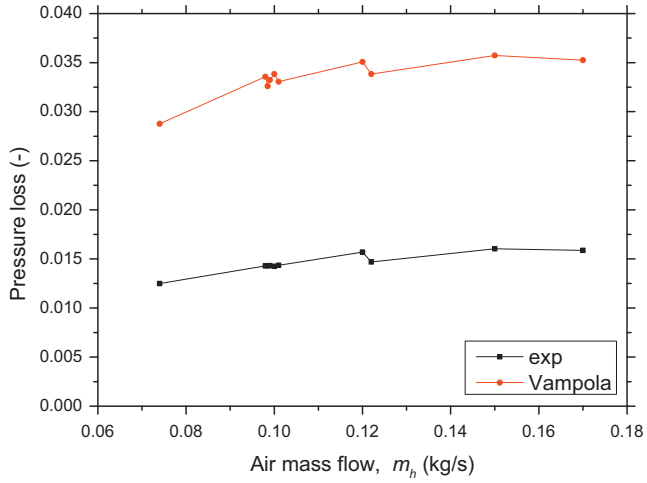

Fig. 5. Experimental and calculated pressure loss at different air mass flow.

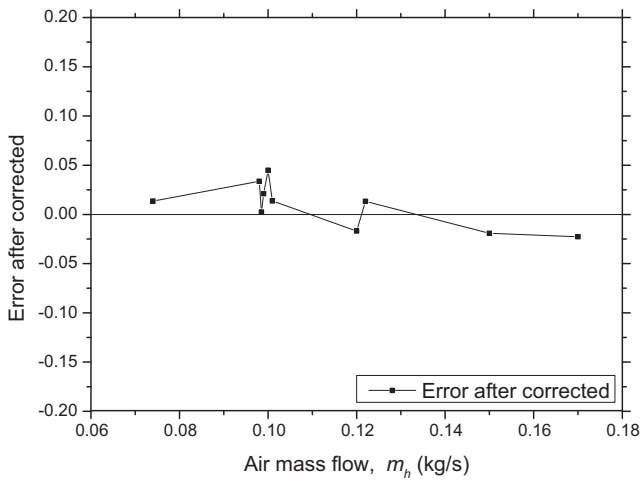

Fig. 6. Pressure loss prediction error of hot side after corrected.

decrease of the elbows and the manufacturing method of brazing. Compared to the ordinary snake tube, tubes with elbows in smaller diameter introduced three additional pressure difference term: (1) additional pressure difference in straight section of tube due to inner diameter decrease, (2) additional pressure difference in elbows due to inner diameter decrease, (3) additional pressure difference due to sudden contraction and expansion at the import and export of elbows. Fig. 7 indicated cold side pressure loss with cold mass flow, where the black present pressure loss calculated by literature, the red present calculated pressure loss after taking the effect of changed diameter of elbows into consideration and the blue is experimental pressure loss. Similar to the hot side pressure loss, there are considerable differences between calculation and experimental data. The difference may be attributed to small diameter of tubes and supercritical pressure of fuel. Some researchers have made efforts on flow resistance characteristics at supercritical pressure (Zhu et al. [31]), however, few research has been carried out when the fuel was heated and under supercritical pressure, so actually pressure loss under these condition can hardly be predicted accurately by conventional correlations such as Blasius and Filonenko.

Based on this, a new correction factor for conventional pressure difference is proposed:

$$f_{c,i} = 1.3 f_i \tag{22}$$

Similar to hot side, the percentage of pressure loss error for cold side is defined as:

$$\text{Cold side pressure loss error} = \frac{\Delta p_{i,cal} - \Delta p_{i,exp}}{\Delta p_{i,exp}} \tag{23}$$

After taking the correction factor into consideration, Fig. 8 shows good agreement between calculation and experiment, with values for all except one test falling below 5% error. The error in mass flow of 0.1 kg/s is larger because the pressure difference is small compared with larger mass flow, hence the relative error of differential pressure transmitter is larger, which influence prediction accuracy.

The two developed correction factors are with small error in pressure loss prediction on both side, which means that they are reasonable and can be referenced when designing flow resistance of finned tube heat exchanger with similar structure

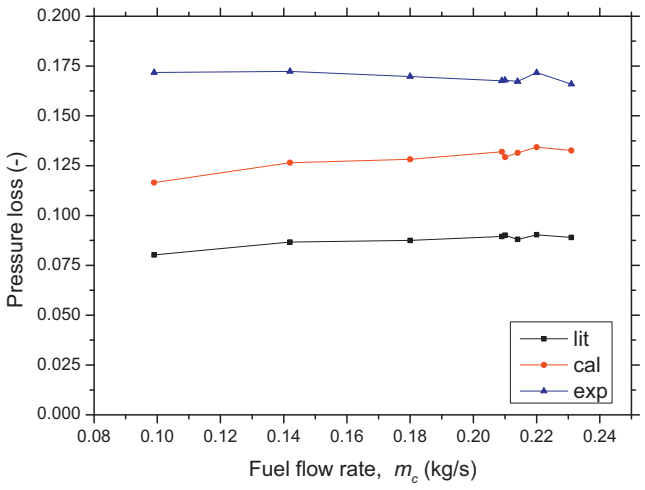

Fig. 7. Literature, calculated and experimental pressure loss at different fuel mass flow.

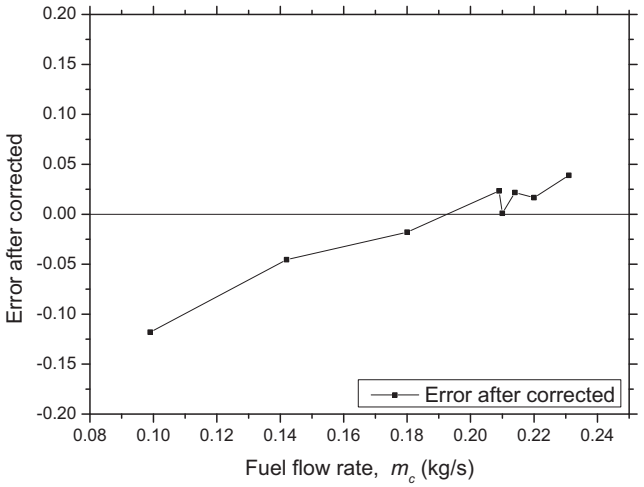

Fig. 8. Pressure loss prediction error of cold side after corrected.

5.2. Heat transfer coefficient

The calculation of heat transfer coefficient of air side has been detailed described in Section 4. Based on calculated heat transfer coefficient, it is found that the heat exchanger was capable of exchanging thermal energy of up to 11.9 kW at LMTD of 57.6 K.

In these experiments, the air-side mass flow range from 0.07 kg/s to 0.17 kg/s, while the mass flow on the fuel side changes from 0.1 kg/s to 0.23 kg/s. Fig. 9 present air-side heat transfer coefficient with different air mass flow under the fuel mass flow of 0.21 kg/s and inlet temperature of 318 K. As can be expected higher velocities result in lower thermal resistance, and air-side heat transfer coefficient increase with the increase of the hot air mass flow, corresponding to total heat transfer coefficient of 274.4 W/m^2 K for Re = 4401 and 172.9 W/m^2 K for Re = 1948.9.

In addition, several experiments have been carried out with the same condition ($\dot{m}_h$ = 0.1 kg/s, $\dot{m}_c$ = 0.21 kg/s, $T_{h,i}$ = 423 K) to ensure the acceptable repeatability. It is found that the air-side heat transfer coefficient error is less than 6%, which means the experimental system is reliable and the heat transfer coefficient is accurate enough.

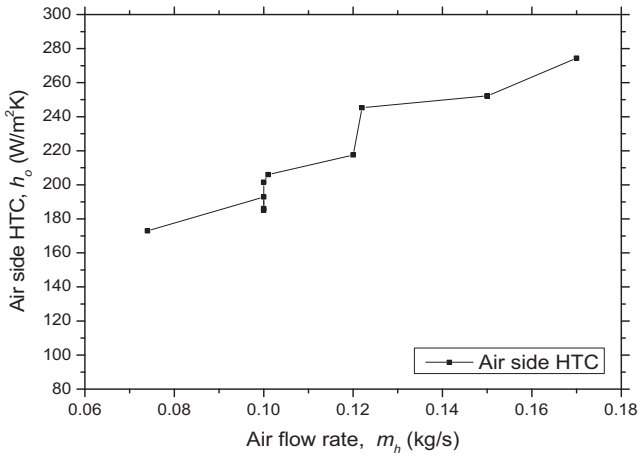

Fig. 9. Air side heat transfer coefficient with air mass flow.

5.3. Finned tube heat transfer empirical correlation

Heat transfer coefficient is crucial in the calculation of heat exchanger dimensions. In order to validate the applicability of experimental correlations to design inline-arranged finned tube heat exchanger, experimental results were compared to literature correlations for finned tube heat transfer.

The heat transfer with finned tube depends on many factors, which are usually grouped into several categories of fluid properties and geometric characteristics. The fluid properties include thermal characteristics such as density and dynamic characteristics such as thermal conductivity and viscosity, which can be expressed with *Re* number and *Pr* number. The geometric parameters include tube outside diameter, fin spacing, fin thickness, longitudinal tube pitch and transverse tube pitch. In general, the outer diameter of tube is assumed as characteristic length in *Nu* number and *Re* number. Table 1 presents the correlations developed for inline arranged finned tube based on a vast number of experimental data. Although some correlations' range does not match the experimental range of this paper, the comparison can be still beneficial.

Comparison between literature predicted values and experimentally obtained values in the form of *Nu* numbers is presented in Fig. 10. It is clearly that experimental *Nu* numbers are lower than predictions. Large discrepancies between literature predictions are also visible. The Vampola correlation gives the largest difference for nearly double the obtained values and the best consistency is obtained for Katz correlations, but still experimental results differ greatly from predictions.

However, the increase of heat transfer coefficient with *Re* number gives a similar trend as the predictions. The difference may be attributed to mass flow and geometric parameter range of experiments. For instance, most of researchers mainly focus on application in refrigeration, so the diameter of tubes is quiet large (as mentioned before, the smallest one is 6mm). Thus flow patterns may be different between various tube diameters. As a result, given correlations are limited in validity to ranges of tube diameter, mass flow and specific working condition.

Refer to form of correlation developed by Groehn, the authors proposed their own empirical correlation using the multiple regression method. The modified empirical relationship for finned tube bundle with small diameter is shown as follow:

$$Nu = 0.161Re^{0.579}Pr^{0.333}\left(\frac{Pr}{Pr_w}\right)^{0.25}$$ valid for $0.6 < Pr < 0.8$ and $1900 < Re < 4500$, where $Re = \frac{G_{max}d_o}{\mu}$ and $Pr = \frac{c_p\mu}{\lambda}$

As shown in Fig. 11, the maximum relative error of fitting is 9.50% and the average relative error is 4.81%; 93.3% points in all experimental results are within 9% error band, which means the developed empirical relationship can be a reliable reference for the design of finned tube heat exchanger with small tube diameter.

Table 1
Literature correlations for inline arranged finned tube heat transfer.

Source	Correlation	Valid for
Schmidt [32]	$Nu = 0.3Re^{0.625}\left(\frac{A_t}{A_0}\right)^{-0.375}Pr^{0.333}$	$5 < \frac{A_t}{A_0} < 12$, $5000 < Re < 10^5$ for high finned tube
Groehn [33]	$Nu = 0.0729Re^{0.74}Pr^{0.36}$	$5000 < Re < 35000$ for low finned tube
Katz et al. [33]	$Nu' = 0.155Re'^{0.6}Pr^{0.333}\left(\frac{\mu}{\mu_w}\right)^{0.14}$ where $Nu' = \frac{h_0d_e}{\lambda}$, $Re' = \frac{\rho u d_e}{\mu}$	For low finned tube
Vampola [30]	$Nu' = 0.251\left(\frac{G_{max}d_e}{\mu}\right)^{0.67}\left(\frac{S_1-d_o}{d_o}\right)^{-0.2}\left(\frac{S_1-d_o}{S}+1\right)^{-0.2}\left(\frac{S_1-d_o}{S_2-d_o}\right)^{0.4}$ where $Nu' = \frac{h_0d_e}{\lambda}$	Not mentioned

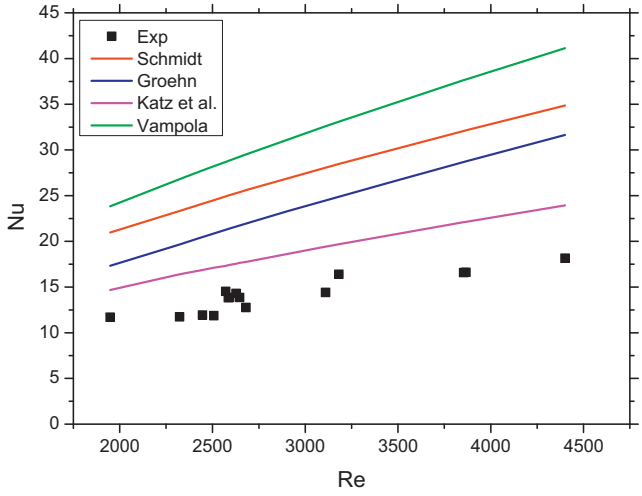

Fig. 10. Comparison between predicted and experimental average Nusselt numbers.

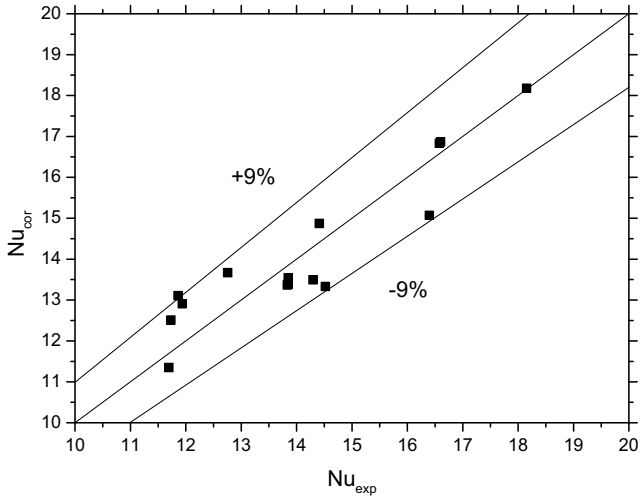

Fig. 11. Predicting error of new empirical correlation.

6. Conclusions

A prototype finned tube heat exchanger intended for potential application in aero-engine was built and tested. The logarithmic mean temperature difference method (LMTD) is used in the heat exchanger design and special manufacture method was detailed introduced. Then the hydraulic performance and heat transfer performance of the heat exchanger was investigated, and the comparison between literature prediction and experimental data was carried out. Some major conclusions are as follow:

(1) A prototype finned tube air-fuel heat exchanger was designed and built, which is both light in weight (1.207 kg) and compact (the heat exchanger surface area density up to 697 m^2/m^3).
(2) Comparisons between literature and experimental data show discrepancies in both pressure difference and heat transfer characteristics. Based on the similar trend of literature and experimental pressure difference changing with mass flow, two correlation factors are proposed to correct the pressure difference.

(3) Experimental data are compared with several empirical correlations for inline arranged finned tube heat transfer, and a new correlation was suggested based on it, predicting the experimental results within 10%.

The authors recommend further detailed study via experiment be carried out to investigate flow and heat transfer characteristics of compact heat exchanger with tubes in minor diameter, so correlations including more geometry parameters can be obtained, and the accuracy of designing finned tube heat exchanger will increase.

References

[1] Y.J. Kim, S.M. Kim, Influence of shaped injection holes on turbine blade leading edge film cooling, Int. J. Heat Mass Transf. 47 (2004) 245–256.
[2] J.C. Han, S. Dutta, S.V. Ekkad, Gas Turbine Heat Transfer and Cooling Technology, Taylor & Francis, New York, 2000.
[3] Rolls-Royce, The Jet Engine, fifth ed., Rolls-Royce plc, Derby, England, 1996.
[4] P. Martini, A. Schulz, H.J. Bauer, Film cooling effectiveness and heat transfer on the trailing edge cutback of gas turbine airfoils with various internal cooling designs, J. Turbomach., Trans. ASME 128 (2006) 196–205.
[5] H. Huang, L.J. Spadaccini, D.R. Sobel, Fuel-cooled thermal management for advanced aeroengines, Trans. ASME 126 (2004) 284–293.
[6] D. Missirlis, K. Yakinthos, A. Palikaras, K. Katheder, A. Goulas, Experimental and numerical investigation of the flow field through a heat exchanger for aero-engine applications, Int. J. Heat Fluid Flow 26 (3) (2005) 440–458, 1.
[7] K. Yakinthos, D. Missirlis, A. Palikaras, P. Storm, B. Simon, A. Goulas, Optimization of the design of recuperative heat exchangers in the exhaust nozzle of an aero engine, Appl. Math. Model. 31 (11) (2007) 2524–2541.
[8] C. Albanakis, K. Yakinthos, K. Kritikos, D. Missirlis, A. Goulas, P. Storm, The effect of heat transfer on the pressure drop through a heat exchanger for aero engine applications, Appl. Therm. Eng. 29 (4) (2009) 634–644.
[9] T. Muszynski, R. Andrzejczyk, Applicability of arrays of microjet heat transfer correlations to design compact heat exchangers, Appl. Therm. Eng. 100 (2016) 105–113.
[10] C.C. Wang, Technology review-a survey of recent patents of fin-and-tube heat exchangers, J. Enhanced Heat Transf. 7 (5) (2000).
[11] C.C. Wang, A survey of recent patents of fin-and-tube heat exchangers from 2001 to 2009, Int. J. Air-Condition. Refrig. 18 (01) (2010) 1–13.
[12] H. Han, Y.L. He, Y.S. Li, Y. Wang, M. Wu, A numerical study on compact enhanced fin-and-tube heat exchangers with oval and circular tube configurations, Int. J. Heat Mass Transf. 65 (2013) 686–695.
[13] X. Liu, J. Yu, G. Yan, A numerical study on the air-side heat transfer of perforated finned-tube heat exchangers with large fin pitches, Int. J. Heat Mass Transf. 100 (2016) 199–207.
[14] C.C. Wang, K.Y. Chi, Heat transfer and friction characteristics of plain fin-and-tube heat exchangers, part I: new experimental data, Int. J. Heat Mass Transf. 43 (15) (2000) 2681–2691.
[15] C.C. Wang, K.Y. Chi, C.J. Chang, Heat transfer and friction characteristics of plain fin-and-tube heat exchangers, part II: correlation, Int. J. Heat Mass Transf. 43 (15) (2000) 2693–2700.
[16] J.Y. Jang, J.Y. Yang, Experimental and 3-D numerical analysis of the thermal-hydraulic characteristics of elliptic finned-tube heat exchangers, Heat Transf. Eng. 19 (4) (1998) 55–67.
[17] Y. Fu, J. Wen, Z. Tao, G. Xu, H. Huang, Surface coking deposition influences on flow and heat transfer of supercritical hydrocarbon fuel in helical tubes, Exp. Therm. Fluid Sci. 85 (2017) 257–265.
[18] Y. Fu, J. Wen, Z. Tao, G. Xu, H. Huang, Experimental research on convective heat transfer of supercritical hydrocarbon fuel flowing through U-turn tubes, Appl. Therm. Eng. 116 (2017) 43–55.
[19] C. Zhang, G. Xu, L. Gao, Z. Tao, H. Deng, K. Zhu, Experimental investigation on heat transfer of a specific fuel (RP-3) flows through downward tubes at supercritical pressure, J. Supercrit. Fluids 72 (2012) 90–99.
[20] A.A. Bhuiyan, A.S. Islam, Thermal and hydraulic performance of finned-tube heat exchangers under different flow ranges: a review on modeling and experiment, Int. J. Heat Mass Transf. 101 (2016) 38–59.
[21] C.C. Wang, R.L. Webb, K.Y. Chi, Data reduction for air-side performance of fin-and-tube heat exchangers, Exp. Therm. Fluid Sci. 21 (4) (2000) 218–226.
[22] J.M. Kay, R.M. Nedderman, 1985. Fluid Mechanics and Transfer Processes. CUP Archive.
[23] S.A. Klein, Engineering Equation Solver (EES), F-Chart Software, Madison, WI.
[24] H.W. Deng, C.B. Zhang, G.Q. Xu, Z. Tao, B. Zhang, G.Z. Liu, Density measurements of endothermic hydrocarbon fuel at sub-and supercritical conditions, J. Chem. Eng. Data 56 (6) (2011) 2980–2986.
[25] H.W. Deng, K. Zhu, G.Q. Xu, Z. Tao, C.B. Zhang, G.Z. Liu, Isobaric specific heat capacity measurement for kerosene RP-3 in the near-critical and supercritical regions, J. Chem. Eng. Data 57 (2) (2011) 263–268.
[26] H.W. Deng, C.B. Zhang, G.Q. Xu, B. Zhang, Z. Tao, K. Zhu, Viscosity measurements of endothermic hydrocarbon fuel from (298 to 788) K under supercritical pressure conditions, J. Chem. Eng. Data 57 (2) (2012) 358–365.
[27] G.Q. Xu, Z.X. Jia, J. Wen, H.W. Deng, Y.C. Fu, Thermal-conductivity measurements of aviation kerosene RP-3 from (285 to 513) K at sub-and supercritical pressures, Int. J. Thermophys. 36 (4) (2015) 620–632.
[28] T.E. Schmidt, Heat transfer calculations for extended surfaces, Refrig. Eng 57 (4) (1949) 351–357.
[29] V. Gnielinski, New equations for heat and mass-transfer in turbulent pipe and channel flow, Int. Chem. Eng. 16 (2) (1976) 359–368.
[30] Meizhong Shi, Zhongzheng Wang, Principle and design of heat exchangers, fifth ed., Southeast University Press, Nanjing, China (in Chinese), 1989.
[31] K. Zhu, G.Q. Xu, Z. Tao, H.W. Deng, Z.H. Ran, C.B. Zhang, Flow frictional resistance characteristics of kerosene RP-3 in horizontal circular tube at supercritical pressure, Exp. Therm. Fluid Sci. 44 (2013) 245–252.
[32] E. Schmidt, Heat Transfer At Fumed Tubes and Computations of Tube Bank Heat Exchangers, Kaltetechnik,No. 4, 15, 98; No. 12, 15, 370, 1963.
[33] E.U. Schlunder, Heat Exchanger Design Handbook, Hemisphere Publishing, New York, NY, 1983.